

Adversarial target-invariant representation learning for domain generalization

Isabela Albuquerque¹ João Monteiro¹ Mohammad Darvishi² Tiago Falk¹ Ioannis Mitliagkas³

Abstract

In contrast to standard assumptions within the empirical risk minimization setting, several applications of machine learning observe distribution shifts across training and test data. As such, a number of domain generalization strategies have been introduced with the goal of achieving good performance on out-of-distribution samples. In this work, we are interested in finding a set of target distributions for which it is possible to guarantee generalization. We show that pair-wise invariance across train distributions ensures invariance to any target domain that can be explained through a mixture of available training domains. We thus present an upper-bound for the risk on the target distribution that depends on a discrepancy measure between pairs of source domains. Following this insight, we introduce an adversarial approach in which pair-wise divergences are estimated and minimized. Experiments on two domain generalization benchmarks for object recognition show that the proposed method yields higher average accuracy on the target domains in comparison to previously introduced adversarial strategies, as well as recently proposed methods based on learning invariant representations.

1. Introduction

One of the most common assumptions in the empirical risk minimization setting is that all examples used for training and testing models are independently and identically drawn from a given distribution. However, in practical scenarios, this assumption can not be taken for granted as there might exist variations between the conditions in which training and test data were collected (Li et al., 2018c). Representative examples can include changes in data acquisition conditions, such as illumination in images for object segmentation, or

new data sources, such as unseen speakers when performing speech recognition, among many others. Previous work has attempted to enable machine learning models to compensate for these mismatch conditions between training and test data distributions under different settings. A popular approach, often referred to as *unsupervised domain adaptation* (Ben-David et al., 2007), relies on access, at training time, to an unlabeled sample from the target test data distribution, to allow for a measure of divergence against the labeled training data to be computed. Several approaches have been introduced with the goal of learning a feature space such that train and unlabeled target data are alike, and classifiers trained on the former will generalize to the latter.

Theoretical results for the domain adaptation setting introduced by Ben-David et al. (2007) showed that under the covariate shift assumption, which considers that labels do not depend on the domain the data was sampled from so that the conditional labels distribution will not shift (Ben-David et al., 2010b), the performance on the target domain is bounded by the performance on the source domain and the \mathcal{H} -divergence (Kifer et al., 2004) between source and target distributions, as measured on a shared feature space. Methods based on such result attempt to learn domain-invariant representations while preserving task-relevant cues (Ganin et al., 2016). Recent adversarial methods for domain adaptation proposed to employ task-specific classifiers in order to align source and target domains (Saito et al., 2018), or augment the loss with a term that penalizes decisions boundaries that cross high-density regions in the learned feature space (Shu et al., 2018).

Despite the success of domain adaptation algorithms in several tasks (Chattopadhyay et al., 2012; Serdyuk et al., 2016; Thompson et al., 2019), such techniques rely on the assumption that an unlabeled sample from a target distribution of interest is known at training time. In this work, on the other hand, we are interested in a more general setting where different *multiple* target distributions are expected at test time and thus *no target unlabeled sample is used during training*. This setting is often referred to as *domain generalization* and has recently drawn attention from the machine learning community. Recent work on domain generalization has included the use data augmentation (Shankar et al., 2018; Volpi et al., 2018) at training time, meta-learning to simulate domain shift (Li et al., 2018a), adding a self-supervised

¹INRS-EMT, Université du Québec, Montreal, Canada.

²Faubert Lab, Université de Montréal, Montreal, Canada. ³Quebec Artificial Intelligence Institute & DIRO, Université de Montréal, Montreal, Canada. Correspondence to: Isabela Albuquerque <isabelamcalbuquerque@gmail.com>.

task to encourage a feature extractor to learn better representations (Carlucci et al., 2019), learning domain-invariant representations (Li et al., 2018c), among other approaches.

In this work, we show that through minimizing pair-wise divergences across a diverse set of training source domains, a feature extractor is encouraged to learn representations which are also invariant across unseen target distributions, under the assumption that target distributions can be explained by a mixture of available sources. We then show that minimizing the highest pair-wise \mathcal{H} -divergence between available source domains encourages the features to be invariant to any such target domain, which enables generalization. We then exploit that property of considered target domains and propose an adversarial algorithm in which one estimates and minimizes pair-wise divergences.

In summary, our main contributions are:

- We revisit and extend results for domain adaptation to the domain generalization case, showing that, under mild assumptions on the possible target distributions, a representation that simultaneously minimizes pair-wise \mathcal{H} -divergences across source domains, will also be encouraged to be invariant considering novel data sources, which induces generalization;
- We devise an adversarial algorithm based on the theoretical results in order to learn representations which are also invariant to new unseen distributions while preserving relevant information for a given task;
- We evaluate the proposed approach on two well-known domain generalization benchmarks and show improvements over state-of-art methods as well as recently introduced approaches.

The remainder of this paper is organized as follows: In Section 2 we define the domain generalization problem and provide results from the domain adaptation literature which will be used in this work. Section 3 presents the related work from the domain generalization literature. In section 4 we describe our setting, present our main results as well as the resulting algorithm. Section 5 provides the experiments description and the respective results. We conclude in Section 6 by presenting the main remarks and future directions.

2. Background and problem setup

Let the data be represented by $\mathcal{X} \subset \mathbb{R}^D$, while labels are given by \mathcal{Y} , which would be $\{0, 1\}$ in the binary case, for instance. Examples correspond to a pair (x, y) , $x \in \mathcal{X}$, $y \in \mathcal{Y}$, such that $y = f(x)$, and $f : \mathcal{X} \rightarrow \mathcal{Y}$ is a deterministic labeling function.

A domain¹ \mathcal{D} is defined as a joint probability distribution over $\mathcal{X} \times \mathcal{Y}$. Moreover, we define a mapping $h : \mathcal{X} \rightarrow \mathcal{Y}$, such that $h \in \mathcal{H}$, where \mathcal{H} is a set of candidate hypothesis, and finally define the risk R associated with a given hypothesis h on domain \mathcal{D} as:

$$R[h] = \mathbb{E}_{x \sim \mathcal{D}} \ell[h(x), f(x)], \quad (1)$$

where the loss $\ell : \mathcal{Y} \times \mathcal{Y} \rightarrow \mathbb{R}_+$ quantifies how different $h(x)$ is from the true labeling function $y = f(x)$ for a given data instance (x, y) .

In the domain generalization setting, one's interest is to train a model h able to minimize the risk on unseen data distributions. Given N_S data sources, we assume that examples $\{x_m^j, y_m^j\}_{m=1}^{M_j}$ for each domain $j \in \{1, \dots, N_S\}$ consist of the only data available during training.

One trivial approach to extend the empirical risk minimization (ERM) setting for domain generalization would be to learn h minimizing the empirical risk $\hat{R}[h]$ measured over all N_S source domains and *hope* generalization would be achieved to the target data, i.e.:

$$h = \arg \min \hat{R} = \frac{1}{N_S} \sum_{j=1}^{N_S} \frac{1}{M_j} \sum_{i=1}^{M_j} \ell[h(x_i), f(x_i)]. \quad (2)$$

In fact, as will be discussed in more detail in next sections, such a rather simplistic approach often yields strong baselines.

2.1. Generalization guarantees domain adaptation

We now state the results from the domain adaptation literature that will be reused in this work. The work of Ben-David et al. (2010a) established the theoretical foundation for studying the cross-domain generalization properties for domain adaptation problems. Based on the covariate shift assumption, which considers that the conditional distribution of the labels over the data does not change across domains, they showed that, given a source domain \mathcal{D}_S and target domain \mathcal{D}_T over a shared feature space, the risk of a given hypothesis h on the target data is bounded by:

$$R_T[h] \leq R_S[h] + d_{\mathcal{H}}[\mathcal{D}_S, \mathcal{D}_T] + \lambda, \quad (3)$$

where λ corresponds to the minimal total risk over both domains which can be achieved within a given hypothesis class \mathcal{H} . The term $d_{\mathcal{H}}[\mathcal{D}_S, \mathcal{D}_T]$ corresponds to the \mathcal{H} -divergence introduced in (Kifer et al., 2004) and defined as follows:

$$d_{\mathcal{H}}[\mathcal{D}_S, \mathcal{D}_T] = 2 \sup_{\eta \in \mathcal{H}} |\Pr_{x \sim \mathcal{D}_S}[\eta(x) = 1] - \Pr_{x \sim \mathcal{D}_T}[\eta(x) = 1]|, \quad (4)$$

¹We use the terms *domain*, *data distribution*, and *data source* interchangeably throughout the text.

where $\eta : \mathcal{X} \rightarrow \{0, 1\}$ is a discriminator responsible for distinguishing examples from \mathcal{D}_S and \mathcal{D}_T . As discussed by Ben-David et al. (2007), an estimate of $d_{\mathcal{H}}[\mathcal{D}_S, \mathcal{D}_T]$ can be directly computed from the error of a binary classifier trained to distinguish domains.

3. Related work

A relatively straightforward approach for achieving generalization across multiple domains is performing empirical risk minimization for the source domains by training a model on all available data sources without any strategies to enforce generalization to the target domains. Using this approach, Li et al. (2017) showed that an AlexNet (Krizhevsky et al., 2012) directly trained on source data from the VLCS (Torralba & Efros, 2011) and PACS (Li et al., 2017) benchmarks is able to reach target accuracy comparable to that of previously proposed domain generalization methods. Follow-up work attempted to build on top of this baseline by using part of the AlexNet as feature extractor and somehow further training it so as to enforce better generalization. In such cases, models are usually composed by a feature extractor, a task classifier, and a module responsible for regularizing the feature extractor in order to impose robustness across different domains. Carlucci et al. (2019), for example, proposed to regularize the feature extractor using a self-supervised task which consists of solving a jigsaw puzzle composed by randomly shuffled patches of each image. The pre-trained feature extractor is thus trained by simultaneously minimizing the task and the self-supervised loss. The proposed approach is referred as JiGen.

The use of a pre-trained neural network as feature extractor was further explored by Li et al. (2019) to learn a domain-agnostic feature extractor along with a classifier. They proposed the so-called episodic training for domain generalization (Epi-FCR) by using domain-specific components to train domain-agnostic ones. More specifically, a domain-agnostic feature extractor model is trained by using domain-specific classifiers, and a domain-agnostic classifier is trained to classify features computed from domain-specific feature extractors. Moreover, Li et al. (2018c) presented an adversarial method for learning invariant representations for domain generalization which does not rely on the covariate shift assumption, but considers that the labels marginal distributions are not “severely” different. More specifically, the authors propose to have a domain classifier specific for each class in order to enforce the feature extractor to learn a feature space where the mismatch between the labels conditional distributions is minimized. The feature extractor is also encouraged to learn domain-invariant features by maximizing the loss provided by a domain classifier that receives as input examples from classes altogether. In order to enforce the features to be informative for the

desired task, the loss of a task classification model is also included in the training of the feature extractor model. This approach is referred in the experiments section as CIDDG.

We further remark that the setting considered herein, to which we refer as *Domain Generalization*, is different with respect to the more well studied *Unsupervised Domain Adaptation*. While in the former one wants to be able to generalize to a specific target distribution defined through an observed unlabeled sample, in the setting we consider no target distribution is given during training. Previous work (Li et al., 2019) included in their experiments an adapted version of an adversarial domain adaption method (Ganin et al., 2016) to problems under the domain generalization setting and showed it can achieve a promising performance. In this contribution we provide a principled way for achieving this.

4. Learning target-agnostic representations for domain generalization

4.1. Setup

We will refer to \mathfrak{D} as a meta-distribution composed by distributions \mathcal{D} denominated domains, i.e., while sampling from \mathfrak{D} , one is actually sampling from one of the possible $\mathcal{D}^i \in \mathfrak{D}$. We further consider that a training set $(x^m, y^m) \sim \mathfrak{D}$ and a test set $(x^{m'}, y^{m'}) \sim \mathfrak{D}$ are constructed, and the set of domains represented in the training and test sets are referred to as source and target domains. The N_S source domains and the N_T target domains are denoted as \mathcal{D}_S^i , $i \in \{1, \dots, N_S\}$, and as \mathcal{D}_T^j , $j \in \{1, \dots, N_T\}$, respectively. Figure 1 illustrates our setting by representing the meta-distribution along with the source and target domains. At training time, sampling from \mathfrak{D} yields a sample from the \mathcal{D}_S ’s, while at test time, drawing samples from \mathfrak{D} might yield samples from new unseen domains.

As discussed in previous Sections, within the domain generalization setting, no information regarding possible target distributions is available at training phase. We thus argue that no-free-lunch type of impossibility results may be used to conclude that it is impossible to generalize to any possible target distribution, so that one must assume something about the target test domain in order to enable generalization. Given that, the approach we take herein is to somehow tie the possible targets with observed sources, which we do by considering the set of target distributions explainable by a mixture of available training domains. Such assumption is also discussed in previous work (Hoffman et al., 2018).

In the following, we discuss direct extensions of previous results to show that such an assumption yields two outcomes: (i)-Pair-wise invariant representations across source domain induce pair-wise invariance across possible targets; (ii)-Generalization to new data from available sources yields

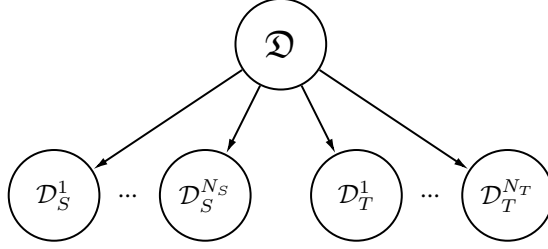


Figure 1: Illustration of the meta-distribution Ω composed by the source and target domains on a domain generalization problem.

generalization to the considered test domains.

Given such results, we thus argue that collecting diverse datasets is yet another factor to consider other than the amount of available data, since that would enable generalization to a larger set of target distributions.

4.2. Invariance on new domains

Let $d_{\mathcal{H}}[\mathcal{D}_S^i, \mathcal{D}_S^k]$ denote the \mathcal{H} -divergence between the i -th and k -th source domains \mathcal{D}_S^i and \mathcal{D}_S^k , and $d_{\mathcal{H}}[\mathcal{D}_S^i, \mathcal{D}_S^k] \leq \epsilon$, $\forall i, k \in \{1, \dots, N_S\}$, where N_S is the number of source domains, and ϵ represents the maximum pair-wise \mathcal{H} -divergence across all source domains. Following Hoffman et al. (2018), we assume that all examples that appear at test time can be explained by a mixture of the source domains, i.e., any target domain \mathcal{D}_T^j can be written as $\mathcal{D}_T^j(\cdot) = \sum_{i=1}^{N_S} \pi_{i,j} \mathcal{D}_S^i(\cdot)$, $\pi_{i,j} \in \Delta_{N_S}$. We now state the proposition that motivates the introduced algorithm.

Proposition 1. *(Bounding the \mathcal{H} -divergence between unseen domains) Given the previous setup and assumptions, the following inequality holds for the \mathcal{H} -divergence between any target domains \mathcal{D}_T^k and \mathcal{D}_T^j :*

$$d_{\mathcal{H}}[\mathcal{D}_T^k, \mathcal{D}_T^j] \leq \min(2, 2\epsilon). \quad (5)$$

Proof. C.f. supplementary material.

Therefore, given the aforementioned assumptions, by minimizing the maximum pair-wise \mathcal{H} -divergence between source domains, we are also minimizing the \mathcal{H} -divergence between possible target domains. Taking such result into account, we propose a method to learn representations by minimizing an empirical estimation of ϵ , while attaining good performance at the goal task.

4.3. Generalizing to unseen domains

In order to show that, under the mixture assumption, minimizing pair-wise \mathcal{H} -divergences leads to better generalization on an unseen target domain, we present a direct extension to our setting of the generalization bound stated

by (Zhao et al., 2018), as a Corollary of their Theorem 2.

Corollary 1. *(Generalization to unseen domains) Given the previous setup and assumptions, the following inequality holds for the risk $R_T^j[h]$ of a given hypothesis h on a target domain \mathcal{D}_T^j :*

$$R_T^j[h] \leq \sum_{i=1}^{N_S} \pi_{i,j} R_S^i[h] + \frac{\epsilon}{2} + \lambda_{\pi_j}, \quad (6)$$

where λ_{π_j} is the risk of the optimal hypothesis on the sources mixture representing \mathcal{D}_T^j .

Proof. C.f. supplementary material.

The result stated in 6 shows that, as the maximum \mathcal{H} -divergence between source domains is minimized, the risk of h on unseen target domains gets closer to a convex combination of the risks observed over training domains.

4.4. Method

We now describe the proposed algorithm for domain generalization by learning pair-wise invariant representations. Motivated by the previous results, which showed that under certain assumptions the \mathcal{H} -divergence between source and target domains is upper-bounded by the maximum pair-wise \mathcal{H} -divergence between all source domains, we propose to directly minimize ϵ , and do so with an adversarial approach that extends previously proposed adversarial single and multi-source domain adaptation methods to the domain generalization setting. Intuitively, we aim at learning a representation space which simultaneously separates the classes for the task at hand, while at the same time distinguishing domains is difficult. Our algorithm contains three main modules: a feature extractor F with parameters ϕ , a task classifier C with parameters θ_C , and a set of \mathcal{H} -divergence estimators D_j with parameters θ_j , $j \in \{1, \dots, N_S\}$.

Different strategies to estimate pair-wise \mathcal{H} -divergences: As shown in (Ben-David et al., 2007), the \mathcal{H} -divergence between two domains can be estimated by a discriminator responsible for distinguishing samples from one domain and the other. In our considered case, however, this could be implemented in different ways. For example, one could have an empirical \mathcal{H} -divergence estimator for each pair of source domains and train the feature extractor to minimize the maximum values across such estimates. However, if this procedure is adopted, the number of \mathcal{H} -divergence estimators is $\mathcal{O}(n^2)$, where $n = N_S$. Another possibility is *one-vs-all*: a model is responsible for discriminating examples from one source domain from all the others. By doing so, each discriminator is thus estimating an average of the empirical \mathcal{H} -divergence between one source domain and the remaining ones. As a result, we have one domain discriminator per source domain,

which corresponds to $\mathcal{O}(n)$ \mathcal{H} -divergence estimators. A third option would be having a discriminator model to tell whether any two input examples belong to the same domain or not. In this simple case, the number of necessary models to estimate ϵ would be $\mathcal{O}(1)$.

Given the three described alternatives, we decided to estimate ϵ using the second approach corresponding to $\mathcal{O}(n)$ discriminators so as to balance computational cost and model capacity. Thus, a training example (x^m, y^m) drawn from the j -th source domain will now correspond to a tuple $(x^m, y_C^m, y_1^m, \dots, y_{N_S}^m)$, where y_C^m corresponds to the task label, and y_k^m is equal to 1 in case $k = j$, or 0 otherwise.

The procedure for estimating ϕ, θ_T , and all θ_j 's can be thus formulated as the following multiplayer minimax game:

$$\begin{aligned} \min_{\phi, \theta_C} \max_{\theta_1, \dots, \theta_{N_S}} & \mathcal{L}_C(C(F(x; \phi); \theta_C), y_C) \\ & - \sum_{j=1}^{N_S} \mathcal{L}_j(D_j(F(x; \phi); \theta_j), y_j), \end{aligned} \quad (7)$$

where \mathcal{L}_C is the task-related loss, and each \mathcal{L}_j represents the loss for the one-versus-all domain binary classification tasks. The training pseudocode can be found in the supplementary material. This minimax game can be seen as the training of the generator on a multiple-discriminator generative adversarial network (GAN) (Durugkar et al., 2016). Intuitively, the feature extractor attempts to minimize $\mathcal{L}_C(\cdot; \theta_C)$ as well as the estimated \mathcal{H} -divergences, which is achieved through the maximization of the losses provided by the domain discriminators, while each domain discriminator aims at improving its estimation of the empirical \mathcal{H} -divergence.

Training is carried out with alternate updates on ϕ, θ_C and all θ_i 's. However, as is well known from the literature, adversarially training the pair task classifier+feature extractor against the discriminators might introduce challenging training instabilities. As such, in order to alleviate this issue, we leverage recently introduced regularization strategies specifically tailored for the multiple discriminator setting. Namely, a random projection layer is introduced to the input of each domain discriminator, as in (Neyshabur et al., 2017; Albuquerque et al., 2019). The dimensionality of the projected data is a hyperparameter, and its tuning includes the option of not projecting the output of the feature extractor. We show in Figure 2 an illustration of the proposed approach.

As a practical remark, adversarial approaches similar to the one proposed here are often employed in domain adaptation, and the minimax game is often reformulated by the introduction of a gradient reversal layer (Ganin et al., 2016) to allow updating all the involved parameters simultaneously. We observed that our method was able to perform well on domain generalization problems without the need for such a trick,

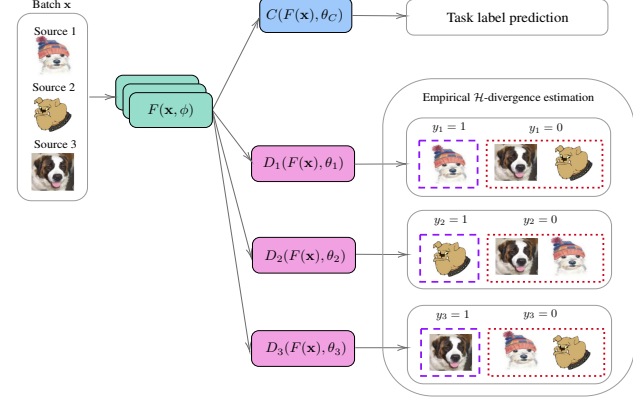


Figure 2: Proposed approach illustration. Training examples from different source domains have different domain labels for each domain discriminator.

and training was generally stable in the sense that most hyperparameters tested converged to a reasonable performance range.

5. Experiments

In this section we provide empirical evidence showing that our method for learning target-domain invariant representations is effective in enabling generalization to novel domains. We perform experiments on the PACS (Li et al., 2017) and VLCS (Fang et al., 2013) domain generalization benchmarks which consist of object recognition tasks. We train models using a *leave-one-domain-out* scheme and compare the best accuracy obtained on the test partition of the target domain data against results obtained by previously proposed domain generalization methods.

Besides the comparison with previously proposed strategies, we further validate that our method achieves better generalization on the target domain when trained with more source domains. This is expected since, as the number of source domains decreases, it becomes harder to represent the target distribution as a combination of the sources. As a consequence, the required assumption for Proposition 1 will not hold, and learning a representation space that minimizes pair-wise \mathcal{H} -divergences on source domains will no longer ensure target invariance. We show that with experiments on the VLCS benchmark using a leave-two-domains-out scheme, and evaluate the performance on a single left out target distribution. We perform further experiments on the PACS benchmark to investigate whether the proposed approach is enforcing pair-wise \mathcal{H} -divergence minimization.

In the last part of our evaluation, we study a practical aspect which appears when models are designed to be used in novel data sources: when to stop training? Evaluation on held-out validation data might be meaningless in this case, and

hence the effect on the resulting performance of employing different stopping criteria is discussed. Results showing the impact of the random projection layer on final performance are discussed in the supplementary material.

5.1. Experimental details

5.1.1. BASELINES

We compare the proposed approach to a model trained using all source domains without any mechanism to enforce domain generalization and with the same architecture. Furthermore, we include the results reported by [Carlucci et al. \(2019\)](#) using the same architecture and training. As these models are trained according to Eq. 2, they are referred in the results tables as ERM. The model of [Carlucci et al. \(2019\)](#) is referred to as ERM-JiGen. Moreover, we consider for comparison the invariant risk minimization (IRM) strategy ([Arjovsky et al., 2019](#)). This approach was included in our experiments due to the fact it also assumes that by ensuring invariance across a diverse set of training domains, one will be able to also generalize to novel target domains. While in ([Arjovsky et al., 2019](#)) it is assumed that invariance can be achieved by ensuring the optimal classifier matches for all training distributions, we explicitly approximate and minimize pair-wise \mathcal{H} -divergences. From a practical perspective, while IRM does not require training N_S discriminators, gradient penalties have to be computed for the feature extractor, which is not needed in our proposed setting.

We also include the performance of different methods as reported in the literature. Epi-FCR ([Carlucci et al., 2019](#)), JiGen ([Li et al., 2019](#)), and CCSA ([Motiian et al., 2017](#)) were considered, along with adversarial approaches such as CIDDG ([Li et al., 2018c](#)) and MMD-AAE ([Li et al., 2018b](#)). Following [Li et al. \(2019\)](#), which adapted DANN for domain generalization, we further report the performance achieved by this method.

5.1.2. IMPLEMENTATION DETAILS

Following previous work on domain generalization ([Li et al., 2017; 2019](#)), we use models pre-trained on the ILSVRC dataset ([Russakovsky et al., 2015](#)) as initialization. For fair comparison, all models we implemented were given a budget of 200 epochs. We use label smoothing ([Szegedy et al., 2016](#)) on the task classifier in order to prevent overfitting. Models were trained using SGD with Polyak’s acceleration. One epoch corresponds to the length of the largest source domain training sample. The learning rate was “warmed-up” for a number of training iterations equal to n_w . Hyperparameter tuning was performed through random search over a pre-defined grid so as to find the best values for the learning rate (lr), momentum, weight decay, label smoothing

Table 1: Classification accuracy for models trained considering leave-one-domain-out validation on the VLCS benchmark.

Target (→)	V	L	C	S	Average
CCSA	67.10	62.10	92.30	59.10	70.15
DANN	66.40	64.00	92.60	63.60	71.70
MMD-AAE	67.70	62.60	94.40	64.40	72.28
Epi-FCR	67.10	64.30	94.10	65.90	72.90
JiGen	70.62	60.90	96.93	64.30	73.19
ERM - JiGen	71.96	59.18	96.93	62.57	72.66
IRM	72.16	62.36	98.35	67.82	75.17
ERM	73.44	60.44	97.88	67.92	74.92
Ours	71.14	67.63	95.52	69.37	75.92

parameter ls , n_w , random projection size², learning rate reduction factor, and weighting (α). Each model was run with three different initializations (random seeds 1, 10, and 100 selected *a priori*) and the average best accuracy on the test partition of the target domain is reported. Details of the hyperparameters grid used in the search are provided in the Appendix³. For our ERM we used the same hyperparameters as in ([Carlucci et al., 2019](#)), while for IRM we employed the same hyperparameter values reported in the authors implementation of the colored MNIST experiments.

5.2. VLCS

The VLCS benchmark is composed by 5 overlapping classes from the VOC2007 ([Everingham et al., 2010](#)), LabelMe ([Russell et al., 2008](#)), Caltech-101 ([Griffin et al., 2007](#)), and SUN ([Choi et al., 2010](#)) datasets. According to results reported in the literature, the most challenging domain for this benchmark is the LabelMe dataset. Therefore, we utilize it as target domain to perform hyperparameter search. In Table 1, we reported the average accuracy on the test partition obtained by our model across three initializations using leave-one-domain-out validation. By observing the results, we first notice that our ERM baseline outperforms all previously reported results, which makes the task of improving on top of this baseline for our adversarial model further challenging. When analyzing the results obtained by the proposed approach, we observe it was able to outperform our ERM baseline in two domains, including the most difficult one. On the other hand, our strategy decreased the accuracy obtained on Caltech101 in comparison to ERM and IRM. When considering previous domain generalization methods, we observe that our approach presented an improved performance in almost all cases.

²The option of not having the random projection layer is included in the grid search.

³Code for reproducing all experiments is available at <https://github.com/belaalb/TI-DG>.

Table 2: Impact of decreasing the number of source domains on VLCS. Rows represent the two source domains used.

Target	Method	Source					
		VC	VL	VS	LC	LS	CS
V	ERM	-	-	-	66.14	72.16	69.89
	Ours	-	-	-	62.39	69.89	67.23
L	ERM	58.32	-	62.11	-	-	59.85
	Ours	65.37	-	65.87	-	-	64.37
C	ERM	-	98.82	98.58	-	84.67	-
	Ours	-	95.75	96.70	-	81.84	-
S	ERM	69.04	66.29	-	59.80	-	-
	Ours	69.54	68.43	-	57.06	-	-

5.2.1. IMPACT OF SOURCE DOMAINS DIVERSITY ON TARGET ACCURACY

In this experiment, we verify whether removing examples from one source domain impacts the performance on the target domain. We evaluate each target domain on models trained using all possible combinations of the remaining domains as sources. The ERM baseline is also included for reference. Results presented in Table 2 show that for all target domains, decreasing the number of source domains from 3 (see Table 1) to 2 hurt the classification performance for almost all combinations of source domains. We notice that in some cases, excluding a particular source from the training severely decreases the target loss. As an example, for the Caltech-101, excluding from training examples from the VOC dataset decreased the accuracy in more than 10% for the proposed approach, as well as for ERM.

5.3. PACS

The object recognition benchmark referred to as PACS consists of images distributed into 7 classes originated from four different datasets: Photo (P), Art painting (A), Cartoon (C), and Sketch (S). According to previous results (*c.f.* Table 3), the Sketch domain presents the lowest accuracy when used as target domain and thus it can be considered the most challenging one. Taking this into account, we tuned our model using this domain as target and reused the same hyperparameters for the experiments with the remaining domains. In Table 3 we show the results obtained by our method averaged over 3 different initializations along with all the compared approaches. Overall, we observe that the proposed method achieves better average performance across all source domains but Photo than ERM and IRM.

5.3.1. ESTIMATING PAIR-WISE \mathcal{H} -DIVERGENCES

We investigate whether cross-domain \mathcal{H} -divergences are being in fact reduced by the proposed approach, and more importantly, we assess if the \mathcal{H} -divergence between the unseen target domain and the sources decreases, in accordance to Proposition 1. To do so, we approximate the \mathcal{H} -divergence

Table 3: Classification accuracy for models trained considering leave-one-domain-out validation on PACS.

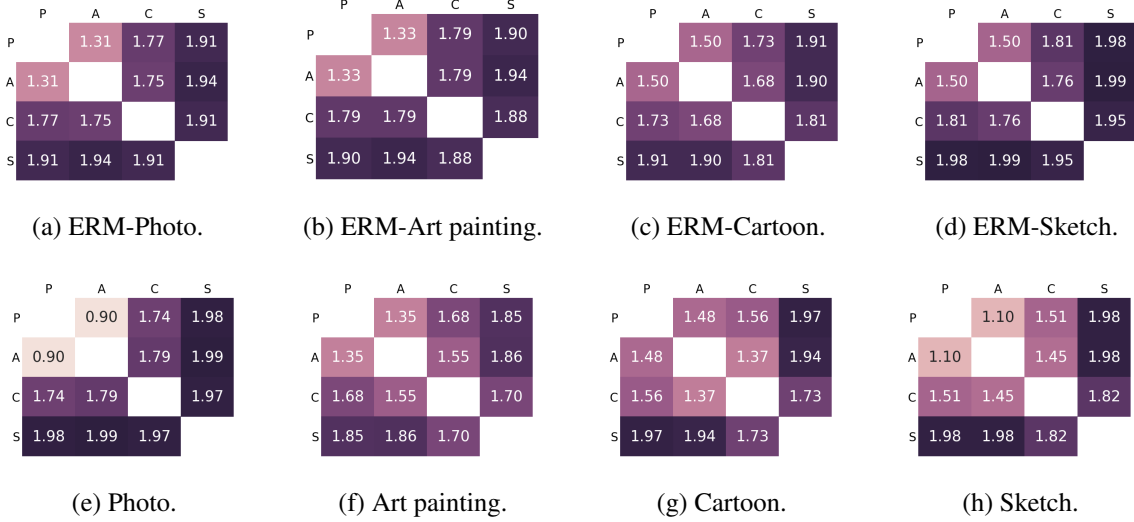
Target (\rightarrow)	P	A	C	S	Average
DANN	88.10	63.20	67.50	57.00	69.00
Epi-FCR	86.10	64.70	72.30	65.00	72.00
JiGen	89.00	67.63	71.71	65.18	73.38
ERM - JiGen	89.98	66.68	69.41	60.02	71.52
IRM	89.97	64.84	71.16	63.63	72.39
ERM	90.02	64.86	70.18	61.40	71.61
Ours	88.12	66.60	73.36	66.19	73.55

by computing the proxy \mathcal{A} -distance (Ben-David et al., 2007) for all pairs of domains for the models obtained with ERM as well as our approach. Results are presented in Figure 3.

We compute the proxy \mathcal{A} -distance by performing domain discrimination for each domain pair on the PACS benchmark considering the representation space learned by the feature extractor from each trained model. We implement the discriminators using tree ensemble classifiers with 100 estimators. We thus report the average classification accuracy using 5-fold cross-validation independently run for each domain pair. Each domain is represented by a random sample of size 500. We present the results in Figure 3. Each entry corresponds to the proxy \mathcal{A} -distance between a pair of domains indicated in the row and the column. Notice that the diagonals are left blank as we do not compute the domain classification accuracy between the same domains. As expected, the proposed algorithm is effective in inducing invariance across pairs of source distributions when compared to ERM, which preserves more domain information given that it is possible to distinguish data sources with higher accuracy in their case.

5.3.2. DOMAIN GENERALIZATION IN PRACTICAL SCENARIOS

Previous experiments report results on an optimistic scenario where target data is available for at least selecting the best performing model. Here, we compare those results with the ones obtained on stopping criteria that only use information from the source domains. One straightforward way to do so consists of selecting the best performing model on the validation partition of the source domains and then finally evaluate it on the target data. However, as previously pointed-out by Innocente & Caputo (2018), this quantity might not be informative in the domain generalization setting. We thus assess the performance of our proposed method considering two stopping criteria: i) validation accuracy on the source domains and ii) training task loss. We report our results in Table 4 alongside the performance reported by Li et al. (2018c) for CIDDG. The same hyperparameters as for the results in Table 3 are used. We notice that, when using the task loss as stopping criterion, our strat-


 Figure 3: Cross-domain proxy \mathcal{A} -distance for models trained on the PACS benchmark using leave-one-domain-out validation.

egy outperforms CIDDG for almost all domains while its performance severely degrades when Sketch is the target. We then repeat the same experiment but now replacing the pre-trained AlexNet by a pre-trained ResNet-18, since this architecture has shown promising results in recent work (Carlucci et al., 2019). ResNet-18 implementation details and hyperparameters are provided in the supplementary material. We compare our approach with JiGen⁴ by adopting the same previous stopping criteria for both methods. We further report in Table 4 the performance obtained by JiGen as reported in (Carlucci et al., 2019), as well as results obtained by Epi-FCR as in (Li et al., 2019), although it is not clear which stopping criterion was adopted for those cases. We observe that replacing AlexNet by ResNet-18 makes our method more robust across varying stopping criteria. On a practical note, we observe that only reporting the performance obtained by the best model on the target domain might hide important aspects, such as the fact that AlexNet presents an unstable training when Sketch is the target. We thus believe that the best methodology to be adopted when analyzing domain generalization strategies is to report their performance across different stopping criteria.

6. Conclusion

We tackled the domain generalization problem and introduced a novel adversarial strategy in order to learn invariant representations across new distributions. Our method is motivated by the presented results which showed that, under mild assumptions over possible target domains, a feature space where pair-wise \mathcal{H} -divergences on the source domains

⁴Results are generated using the original JiGen implementation.

Table 4: Classification accuracy obtained considering different stopping criteria with AlexNet and ResNet-18.

Method (↓)	Criterion (↓)	P	A	C	S	Average
AlexNet						
Ours	Source acc.	85.33	57.76	69.71	49.45	65.56
Ours	Source loss	87.37	66.70	70.26	50.98	68.82
Ours	Target acc.	88.80	66.70	73.29	65.03	73.45
CIDDG	(Li et al., 2018c)	78.65	62.70	69.73	64.45	68.88
ResNet-18						
Ours	Source acc.	93.70	79.22	76.34	75.14	81.10
Ours	Source loss	93.75	77.78	75.54	77.58	81.16
Ours	Target acc.	94.63	81.44	79.35	79.52	83.34
Ours	Source acc.	95.83	78.52	73.31	69.14	79.20
JiGen	Source loss	95.83	78.89	73.32	70.73	79.69
JiGen	Target acc.	96.11	79.56	74.25	71.00	80.23
Epi-FCR	(Carlucci et al., 2019)	96.03	79.42	75.25	71.35	80.51
Epi-FCR	(Li et al., 2019)	93.90	82.10	77.00	73.00	81.50

are minimized induces small divergences across any two target domains, thus yielding generalization. Our approach employs a multiple discriminator setting such that pair-wise divergences are efficiently estimated, while a feature extractor aims at minimizing such mismatches. A practical conclusion one can draw from our results regards the need for diverse datasets so as to enable the mixture assumption to hold. We thus believe that a relevant factor to be considered when collecting new datasets, besides the amount of data, is the within class diversity, so that the set of target distributions which can be defined satisfying the mixture assumption becomes larger. Moreover, we remark that different stopping criteria have to be considered since no meaningful indicator of generalization is available if no out-of-distribution data is available during training. Since we found different models to be more or less robust to different criteria, our conclusion is therefore that future contributions on the type of problems we consider should report results

under multiple criteria, as discussed in Section 5.3.2. Other strategies not explored herein might also be considered, such as entirely leaving one domain out for performing validation when enough domains are given for training.

References

Albuquerque, I., Monteiro, J., Doan, T., Considine, B., Falk, T., and Mitliagkas, I. Multi-objective training of generative adversarial networks with multiple discriminators. In *International Conference on Machine Learning*, pp. 202–211, 2019.

Arjovsky, M., Bottou, L., Gulrajani, I., and Lopez-Paz, D. Invariant risk minimization. *arXiv preprint arXiv:1907.02893*, 2019.

Ben-David, S., Blitzer, J., Crammer, K., and Pereira, F. Analysis of representations for domain adaptation. In *Advances in neural information processing systems*, pp. 137–144, 2007.

Ben-David, S., Blitzer, J., Crammer, K., Kulesza, A., Pereira, F., and Vaughan, J. W. A theory of learning from different domains. *Machine learning*, 79(1-2):151–175, 2010a.

Ben-David, S., Lu, T., Luu, T., and Pál, D. Impossibility theorems for domain adaptation. In *International Conference on Artificial Intelligence and Statistics*, pp. 129–136, 2010b.

Carlucci, F. M., D’Innocente, A., Bucci, S., Caputo, B., and Tommasi, T. Domain generalization by solving jigsaw puzzles. In *Proceedings of the IEEE Conference on Computer Vision and Pattern Recognition*, pp. 2229–2238, 2019.

Chattopadhyay, R., Sun, Q., Fan, W., Davidson, I., Panchanathan, S., and Ye, J. Multisource domain adaptation and its application to early detection of fatigue. *ACM Transactions on Knowledge Discovery from Data (TKDD)*, 6(4):18, 2012.

Choi, M. J., Lim, J. J., Torralba, A., and Willsky, A. S. Exploiting hierarchical context on a large database of object categories. In *2010 IEEE Computer Society Conference on Computer Vision and Pattern Recognition*, pp. 129–136. IEEE, 2010.

Durugkar, I., Gemp, I., and Mahadevan, S. Generative multi-adversarial networks. *arXiv preprint arXiv:1611.01673*, 2016.

DInnocente, A. and Caputo, B. Domain generalization with domain-specific aggregation modules. In *German Conference on Pattern Recognition*, pp. 187–198. Springer, 2018.

Everingham, M., Van Gool, L., Williams, C. K., Winn, J., and Zisserman, A. The pascal visual object classes (voc) challenge. *International journal of computer vision*, 88(2):303–338, 2010.

Fang, C., Xu, Y., and Rockmore, D. N. Unbiased metric learning: On the utilization of multiple datasets and web images for softening bias. In *Proceedings of the IEEE International Conference on Computer Vision*, pp. 1657–1664, 2013.

Ganin, Y., Ustinova, E., Ajakan, H., Germain, P., Larochelle, H., Laviolette, F., Marchand, M., and Lempitsky, V. Domain-adversarial training of neural networks. *The Journal of Machine Learning Research*, 17(1):2096–2030, 2016.

Griffin, G., Holub, A., and Perona, P. Caltech-256 object category dataset. 2007.

He, K., Zhang, X., Ren, S., and Sun, J. Deep residual learning for image recognition. In *Proceedings of the IEEE conference on computer vision and pattern recognition*, pp. 770–778, 2016.

Hoffman, J., Mohri, M., and Zhang, N. Algorithms and theory for multiple-source adaptation. In *Advances in Neural Information Processing Systems*, pp. 8246–8256, 2018.

Kifer, D., Ben-David, S., and Gehrke, J. Detecting change in data streams. In *Proceedings of the Thirtieth international conference on Very large data bases-Volume 30*, pp. 180–191. VLDB Endowment, 2004.

Krizhevsky, A., Sutskever, I., and Hinton, G. E. Imagenet classification with deep convolutional neural networks. In *Advances in neural information processing systems*, pp. 1097–1105, 2012.

Li, D., Yang, Y., Song, Y.-Z., and Hospedales, T. M. Deeper, broader and artier domain generalization. In *Proceedings of the IEEE International Conference on Computer Vision*, pp. 5542–5550, 2017.

Li, D., Yang, Y., Song, Y.-Z., and Hospedales, T. M. Learning to generalize: Meta-learning for domain generalization. In *Thirty-Second AAAI Conference on Artificial Intelligence*, 2018a.

Li, D., Zhang, J., Yang, Y., Liu, C., Song, Y.-Z., and Hospedales, T. M. Episodic training for domain generalization. *arXiv preprint arXiv:1902.00113*, 2019.

Li, H., Jialin Pan, S., Wang, S., and Kot, A. C. Domain generalization with adversarial feature learning. In *Proceedings of the IEEE Conference on Computer Vision and Pattern Recognition*, pp. 5400–5409, 2018b.

Li, Y., Tian, X., Gong, M., Liu, Y., Liu, T., Zhang, K., and Tao, D. Deep domain generalization via conditional invariant adversarial networks. In *Proceedings of the European Conference on Computer Vision (ECCV)*, pp. 624–639, 2018c.

Motiian, S., Piccirilli, M., Adjerooh, D. A., and Doretto, G. Unified deep supervised domain adaptation and generalization. In *Proceedings of the IEEE International Conference on Computer Vision*, pp. 5715–5725, 2017.

Neyshabur, B., Bhojanapalli, S., and Chakrabarti, A. Stabilizing gan training with multiple random projections. *arXiv preprint arXiv:1705.07831*, 2017.

Russakovsky, O., Deng, J., Su, H., Krause, J., Satheesh, S., Ma, S., Huang, Z., Karpathy, A., Khosla, A., Bernstein, M., Berg, A. C., and Fei-Fei, L. ImageNet Large Scale Visual Recognition Challenge. *International Journal of Computer Vision (IJCV)*, 115(3):211–252, 2015. doi: 10.1007/s11263-015-0816-y.

Russell, B. C., Torralba, A., Murphy, K. P., and Freeman, W. T. Labelme: a database and web-based tool for image annotation. *International journal of computer vision*, 77(1-3):157–173, 2008.

Saito, K., Watanabe, K., Ushiku, Y., and Harada, T. Maximum classifier discrepancy for unsupervised domain adaptation. In *Proceedings of the IEEE Conference on Computer Vision and Pattern Recognition*, pp. 3723–3732, 2018.

Serdyuk, D., Audhkhasi, K., Brakel, P., Ramabhadran, B., Thomas, S., and Bengio, Y. Invariant representations for noisy speech recognition. *arXiv preprint arXiv:1612.01928*, 2016.

Shankar, S., Piratla, V., Chakrabarti, S., Chaudhuri, S., Jyothi, P., and Sarawagi, S. Generalizing across domains via cross-gradient training. In *International Conference on Learning Representations*, 2018. URL <https://openreview.net/forum?id=r1Dx7fbCW>.

Shu, R., Bui, H. H., Narui, H., and Ermon, S. A dirt-t approach to unsupervised domain adaptation. In *Proc. 6th International Conference on Learning Representations*, 2018.

Szegedy, C., Vanhoucke, V., Ioffe, S., Shlens, J., and Wojna, Z. Rethinking the inception architecture for computer vision. In *Proceedings of the IEEE conference on computer vision and pattern recognition*, pp. 2818–2826, 2016.

Thompson, B., Gwinnup, J., Khayrallah, H., Duh, K., and Koehn, P. Overcoming catastrophic forgetting during domain adaptation of neural machine translation. In *Proceedings of the 2019 Conference of the North American Chapter of the Association for Computational Linguistics: Human Language Technologies, Volume 1 (Long and Short Papers)*, pp. 2062–2068, 2019.

Torralba, A. and Efros, A. Unbiased look at dataset bias. In *Proceedings of the 2011 IEEE Conference on Computer Vision and Pattern Recognition*, pp. 1521–1528. IEEE Computer Society, 2011.

Volpi, R., Namkoong, H., Sener, O., Duchi, J. C., Murino, V., and Savarese, S. Generalizing to unseen domains via adversarial data augmentation. In *Advances in Neural Information Processing Systems*, pp. 5334–5344, 2018.

Zhao, H., Zhang, S., Wu, G., Moura, J. M., Costeira, J. P., and Gordon, G. J. Adversarial multiple source domain adaptation. In *Advances in Neural Information Processing Systems*, pp. 8559–8570, 2018.

Zhao, H., Des Combes, R. T., Zhang, K., and Gordon, G. On learning invariant representations for domain adaptation. In *International Conference on Machine Learning*, pp. 7523–7532, 2019.

A. Proof of Proposition 1

Using the triangle inequality for the \mathcal{H} -distance (Zhao et al., 2019) and the fact that $d_{\mathcal{H}}[\mathcal{D}_T^j, \mathcal{D}_S^i] \leq \epsilon, \forall i \in \{1, \dots, N_S\}$ by the triangle inequality as well, we have that for any target domains \mathcal{D}_T^k and \mathcal{D}_T^j ,

$$d_{\mathcal{H}}[\mathcal{D}_T^k, \mathcal{D}_T^j] \leq d_{\mathcal{H}}[\mathcal{D}_T^k, \mathcal{D}_S^i] + d_{\mathcal{H}}[\mathcal{D}_S^i, \mathcal{D}_T^j] \leq \epsilon + \epsilon = 2\epsilon. \quad (8)$$

As the \mathcal{H} -divergence is bounded in $[0, 2]$ the inequality becomes $d_{\mathcal{H}}[\mathcal{D}_T^k, \mathcal{D}_T^j] \leq \min(2, 2\epsilon)$. \square

B. Proof of Corollary 1

Our result is a simple extension of the bound stated by Zhao et al. (2018), which showed that the following inequality holds for the risk $R_T^k[h]$ of a given hypothesis h on a target domain \mathcal{D}_T^j :

$$R_T^j[h] \leq \sum_{i=1}^{N_S} \pi_{i,j} \left(R_S^i[h] + \frac{1}{2} d_{\mathcal{H}}[\mathcal{D}_T^j, \mathcal{D}_S^i] \right) + \lambda_{\pi_j}, \quad (9)$$

where λ_{π_j} is the risk of the optimal hypothesis on the sources mixture $\sum_{i=1}^{N_S} \pi_{i,j} \mathcal{D}_S^i(\cdot)$. If one then includes the mixture assumption over the target domain, i.e. $\mathcal{D}_T^j(\cdot) = \sum_{i=1}^{N_S} \pi_{i,j} \mathcal{D}_S^i(\cdot)$, and further assumes $d_{\mathcal{H}}[\mathcal{D}_S^i, \mathcal{D}_S^k] \leq \epsilon, \forall i, k \in \{1, \dots, N_S\}$, then, by the triangle inequality for $d_{\mathcal{H}}[\cdot, \cdot]$, $d_{\mathcal{H}}[\mathcal{D}_T^j, \mathcal{D}_S^i] \leq \epsilon, \forall i \in \{1, \dots, N_S\}$ and Eq. 9 can be rewritten as:

$$R_T^j[h] \leq \sum_{i=1}^{N_S} \pi_{i,j} R_S^i[h] + \frac{\epsilon}{2} + \lambda_{\pi_j}. \quad (10)$$

\square

C. Pseudocode

Algorithm 1 Adversarial target-invariant representation learning training

```

1: Requires: classifier and feature extractor learning rate ( $\gamma_C$ ), domain discriminators learning rate ( $\gamma_D$ ), scaling ( $\alpha$ ), mini-batch size ( $m$ ).
2: Initialize  $\phi, \theta_C, \theta_1, \dots, \theta_{N_S}$  as  $\phi^0, \theta_C^0, \theta_1^0, \dots, \theta_{N_S}^0$ .
3: for  $t = 1, \dots, \text{number of iterations}$  do
4:   Sample one mini-batch from each source domain  $\{(x_1^i, y_C^i, y_1^i, \dots, y_{N_S}^i)\}_{i=1}^m$ 
5:   # Update domain discriminators
6:   for  $j = 1, \dots, N_S$  do
7:      $\theta_j^t \leftarrow \theta_j^{t-1} + \frac{\gamma_D}{N_S \cdot m} \sum_{i=1}^{N_S \cdot m} \nabla_{\theta_j} \mathcal{L}_j(D_j(F(x^i; \phi^{t-1}); \theta_j^{t-1}), y_j^i)$ 
8:   end for
9:   # Update task classifier
10:   $\theta_C^t \leftarrow \theta_C^{t-1} + \frac{\gamma_C}{N_S \cdot m} \sum_{i=1}^{N_S \cdot m} \nabla_{\theta_C} \mathcal{L}_C(C(F(x^i; \phi^{t-1}); \theta_C^{t-1}), y_C^i)$ 
11:  # Update feature extractor
12:   $\phi^t \leftarrow \phi^{t-1} + \frac{\gamma_C}{N_S \cdot m} (\sum_{i=1}^{N_S \cdot m} \alpha \nabla_{\phi} \mathcal{L}_C(C(F(x^i; \phi^{t-1}); \theta_C^{t-1}), y_C^i) - (1 - \alpha) \nabla_{\theta_j} \mathcal{L}_j(D_j(F(x^i; \phi^{t-1}); \theta_j^t), y_j^i))$ 
13: end for

```

D. Effect of random projection size

We further investigate the effectiveness on providing a more stable training of the random projection layer in the input of each discriminator. For that, we run experiments with 7 different projection sizes, as well as directly using the output of the feature extractor model. Besides the random projection size, we use the same hyperparameters values (the same used in the previous experiment) and initialization for all models. We report in Figure 4 the best target accuracy achieved with all random projection sizes on the PACS benchmark considering the Sketch dataset as target domain. Overall, we observed that

the random projection layer has indeed an impact on the generalization of the learned representation and that the best result was achieved with a size equal to 1000. Moreover, we notice that, in this case, having a smaller (500) random projection layer is less hurtful for the performance than using a larger one. We also found that removing the random projection layer did not allow the training to converge with this experimental setting.

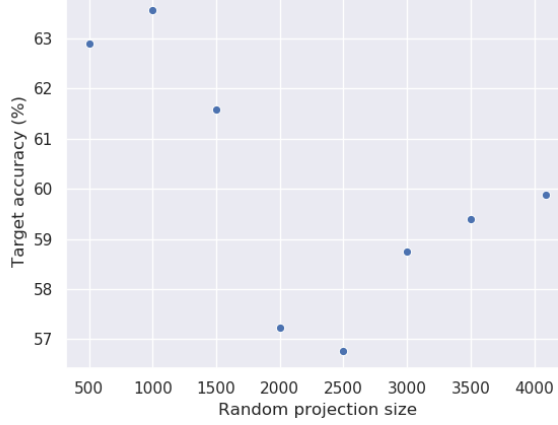


Figure 4: Accuracy obtained on the PACS benchmark using Sketch as target domain.

E. Architectures

In order to obtain a consistent comparison with the aforementioned baseline models, we follow previous work and employ the weights of a pre-trained AlexNet (Krizhevsky et al., 2012) and ResNet-18 (He et al., 2016) as the initialization for the feature extractor model on the experiments. The last layer is discarded and the representation of size 4096 for AlexNet and 512 for ResNet-18 is used as input for the task classifier and the domain discriminators. The domain discriminator architecture with AlexNet, consists of a four-layer fully-connected neural network of size $4096 \rightarrow$ random projection size $\rightarrow 1024 \rightarrow 1$ and five-layer fully connected network of size $512 \rightarrow$ random projection size $\rightarrow 512 \rightarrow 256 \rightarrow 1$ for ResNet-18. The random projection layer is implemented as a linear layer with weights normalized to have unitary L2-norm. The task classifier is a one-layer fully-connected network of size $4096 \rightarrow$ number of classes in the case of AlexNet and $512 \rightarrow$ number of classes in the case of ResNet.

F. Domain generalization benchmarks

The VLCS benchmark is composed by 4 datasets with 5 common classes, namely, bird, car, chair, dog, and person. The number of data points per dataset is detailed as follows. We split each dataset in 80%/20% train/test partitions.

- Pascal VOC2007: 3376;
- LabelMe: 2656;
- Caltech-101: 1415;
- SUN09: 3282.

The PACS benchmark is composed by 4 datasets with 7 common classes, namely, dog, elephant, giraffe, guitar, horse, house, and person. The number of data points per dataset is detailed as follows. We use the original train/validation partitions provided by the benchmark authors.

- Photos: 1670;

- Art painting: 2048;
- Cartoon: 2344;
- Sketch: 3929.

G. Experimental details

The grids used on the hyperparameter search for each hyperparameter are presented in the following. A budget of 200 runs was considered and for each combination of hyperparameters each model was trained for 200 and 30 epochs in the case of AlexNet and ResNet-18, respectively. The best hyperparamters values for AlexNet on PACS and VLCS benchmarks are respectively denoted by $*$, \dagger . For the ResNet-18 experiments on PACS we indicate the hyperparameters by $^+$. Moreover, in the case of ResNet-18, we aggregated the discriminators losses by computing the corresponding hypervolume as in (Albuquerque et al., 2019), with a nadir slack equal to 2.5. All experiments were run considering a minibatch size of 64 (training each iteration took into account 64 examples from each source domain) on single GPU hardware (either an NVIDIA V100 or NVIDIA GeForce GTX 1080Ti).

- Learning rate for the task classifier and feature extractor: $\{0.01^{*,+}, 0.001^\dagger, 0.0005\}$;
- Learning for the domain classifiers: $\{0.0005^*, 0.001, 0.005^{\dagger,+}\}$;
- Weight decay: $\{0.0005^*, 0.001, 0.005^{\dagger,+}\}$;
- Momentum: $\{0.5, 0.9^{*,\dagger,+}\}$;
- Label smoothing: $\{0.0^+, 0.1, 0.2^{*,\dagger}\}$;
- Losses weighting (α): $\{0.35, 0.8^{*,\dagger,+}\}$;
- Random projection size: $\{1000^*, 3000, 3500^\dagger, \text{None}^+\}$;
- Task classifier and feature extractor learning rate warm-up iterations: $\{1, 300^{*,\dagger}, 500^+\}$;
- Warming-up threshold: $\{0.00001^*, 0.0001^{\dagger,+}, 0.001\}$;
- Learning rate schedule patience: $\{25^+, 60^\dagger, 80^*\}$;
- Learning rate schedule decay factor: $\{0.1^+, 0.3^\dagger, 0.5^*\}$.